

Received August 30, 2019, accepted September 30, 2019, date of publication November 1, 2019,
date of current version November 20, 2019.

Digital Object Identifier 10.1109/ACCESS.2019.2950886

Low-Power Wireless With Denseness: The Case of an Electronic Shelf Labeling System—Design and Experience

JINWOO OCK¹, HONGCHAN KIM¹, HYUNG-SIN KIM²,
JEONGYEUP PAEK³, (Senior Member, IEEE), AND
SAEWOONG BAHK¹, (Senior Member, IEEE)

¹Department of Electrical and Computer Engineering, Seoul National University and INMC, Seoul 08826, South Korea

²Department of Electrical Engineering and Computer Science, University of California, Berkeley, CA 94720, USA

³School of Computer Science and Engineering, Chung-Ang University, Seoul 06974, South Korea

Corresponding authors: Jeongyeup Paek (jpaek@cau.ac.kr) and Saewoong Bahk (sbahk@snu.ac.kr)

This work was supported in part by the Bio-Mimetic Robot Research Center Funded by the Defense Acquisition Program Administration, and by the Agency for Defense Development under Grant UD190018ID, in part by the Institute of Information and Communications Technology Planning and Evaluation (IITP) grant funded by the Korea government (MSIT) under Grant 2018-11-1864, Scalable Spectrum Sharing for Beyond 5G Communication, and in part by the Chung-Ang University Research Grants in 2018.

ABSTRACT One of the most important and recurrent tasks in managing a store is to provide accurate information of products to customers by maintaining up-to-date price tags of every item. Till today, however, updating price tags is done manually in most markets, which is labor-intensive, time-consuming, and error-prone. Adopting wirelessly reconfigurable electronic price tags could be of significant benefit to this problem. A key requirement of such a system, then, is to establish a robust, reliable, and scalable wireless communication network while spending minimal energy on thousands of densely-deployed and battery-powered price tags. In this work, we present a comprehensive study of electronic shelf labeling (ESL) system including its design and real-world deployment experiences. While the overall design turns out to be relatively straightforward, our preliminary study using 1000 real commercial e-tags reveals technical challenges in reliable and low-power wireless communication with *ultra-high node density* in *scatter-rich* indoor environments. To address the problem, we adopt multi-radio and multi-channel diversity techniques which need to modify only the gateways but significantly improve overall system performance. Our evaluation from a real-world deployment of 550 tags at an actual convenience store shows that our proposal achieves 98.51% network connectivity, 590 ms average latency for price updates, and over 5 years of e-tag lifetime. ESL system is part of the upcoming smart market era, and we see this work as a practical industrial application case study of Internet of Things technologies.

INDEX TERMS Electronic shelf label, smart market, Internet of Things, IEEE 802.15.4, wireless sensor network, multipath fading, channel diversity.

I. INTRODUCTION

Point-of-sale (POS) terminals, electronic cash registers, computers, bar-code scanners, and many other products are being used today to automate the retail business. One difficult-to-automate process, however, is ensuring that the prices shown on store shelves agree with those displayed and registered at the checkout counter. In most supermarkets, paper price

The associate editor coordinating the review of this manuscript and approving it for publication was Ting Yang.

labels are still manually applied to shelves and display areas. This process leaves much to be desired because it is a costly, labor-intensive, and error-prone operation.

Latest low-power embedded wireless sensor networking technologies have the potential to automate various tedious tasks which have so far been done manually [1]–[3]. *Electronic shelf labeling (ESL)* system is a killer industrial application where a traditional paper price tag is replaced by an electronic price tag (e-tag) with a low-power display (e.g., electronic paper) and a low-power wireless module

(e.g., IEEE 802.15.4), resulting in reliable and convenient (near real-time) remote price updates [4]–[7]. By adopting an *ESL* system, retailers avoid mistagging errors, printing cost, and labor cost coming from manual tagging. Given high marketability with tons of price tags in the world, the industry such as M^2 Communication, LG Innotek, and Pricer has shown great interest in *ESL*. Along with the ongoing effort in industry, addressing technical challenges and design principles for *ESL* systems is worthwhile as research community.

This work presents a comprehensive study of *ESL* system including identifying application requirements, designing a holistic wireless IoT system, and validating the system in a real store with a large number of e-tags. The goal is to provide an *ESL* system solution which reliably works with thousands of e-tags in a small convenience store, not only for small stores themselves but also as a building block for a larger store deployment (e.g., Walmart and Whole Foods).

From our in-lab pilot study with 1000 e-tags of an existing commercial *ESL* system, it is identified, almost always, that a few e-tags are disconnected from the gateway even at close distance. The disconnection period is significantly long and interestingly, becomes longer at the night-time than the day-time. An elaborate analysis unveils that the devil is in the combination of extremely *high node density* and *multipath fading*: E-tags are very densely deployed at metal shelves, some of which are always located at *deep fading holes* where multipath signals interfere destructively [8]. Wireless channel condition is more stable during the night-time, locking an e-tag in a *deep fading hole* for a long time.

E-tags suffering deep fades experience unacceptably long latencies for price updates, and these *only a few* e-tags bring all the complaints from retailers and customers, severely harming the applicability of the entire *ESL* system. To alleviate the problem, we adopt multi-radio and channel diversity techniques, those that are well known in the wireless communication theory but often overlooked in real system implementations, to design a *production-ready ESL* system. In contrast to prior work [9]–[11], proposed schemes require modifying only the gateway of an existing system, which is much more practical than redeploying thousands of e-tags. Our in-store evaluation with 550 tags shows that these diversity techniques improve network connectivity from 17.76% to 98.51% with 99.94% average node connectivity, resulting in reliable price update within 2 seconds, 590 ms on average. The contributions of this work are threefold:

- We design and build a *holistic, production-ready ESL* system, including e-tag and gateway hardware, system architecture, and network protocol.
- We experimentally identify wireless communication challenges coming from *multipath fading* when connecting thousands of nodes *densely* deployed in a *scatter-rich* indoor environment, which confirms wireless channel theory and provides practical lessons learned for researchers.
- Based on the findings, we adopt a solution that nearly eliminates the problem in a real store deployment with

550 e-tags, verifying that diversity techniques are necessary for robust and reliable communication in a dense low-power network with a large number of devices.

We by no means are claiming that each of the techniques and ideas used in our system are novel by themselves. They are adopted from well-known wireless communication theory and prior researches. However, our contribution is in identifying the problem in a real environment, a problem that was occurring in a real commercial system but hard to find and easy to overlook. Once the problem is pin-pointed, solution was straight-forward. Furthermore, our 550~1000 node deployments have much higher node density and scale than any other low-power wireless network testbed [12], which also gives unique value to our study.

The remainder of this paper is organized as follows. We first provide detailed system and network protocol design of *ESL* in Section III, along with its parameter selection and lifetime estimation in Section IV. In Section V, with the observation throughout preliminary experimental studies, we describe the proposed enhancements to our system. We then present the evaluation results in Section VI. We discuss related work in Section II, and conclude the paper in Section VII.

II. RELATED WORK

A pioneering work on ESL is the ‘electronic price label (EPL)’ by Evans *et al.* [5]. EPL features two-way communication between a controller and electronic price labels to ensure price accuracy and reliability similar to ours. However, its evaluation is quite limited with only a few nodes, and does not consider variability of wireless links in real-world markets nor present long-term statistics on the wireless channel conditions. These are the real-world challenges that has been identified and addressed in our work. Yu *et al.* proposed ‘electronic intelligent tag’ [6], which only focuses on the hardware architecture and design without providing details on the implementation nor wireless performance. Kim *et al.* suggested MarketNet for ESL [7] but investigated only the network aspect without using real e-tags. Furthermore, although experiments are performed in a real-world market, only 30 nodes are used, too little to represent the number of e-tags even in a small store. Inspired by but contrary to prior work, the unique contribution of our work is to question the wireless communication aspect of ESL system in an *ultra-dense, indoor* large-scale IoT network, performance evaluation both in a lab and a real convenience store with thousands of devices, and identifying the problem. Once the root cause is identified, solution was straight-forward.

Unique challenge of low-power embedded wireless network (such as wireless sensor network (WSN)) mainly comes from the use of resource-constrained hardware [13] which makes implementation and experimental study necessary to confirm or challenge the principles established in mainstream networks. As part of it, Watteyne *et al.* [8] experimentally measured low-power link quality at 2.4 GHz while moving a transmitter slightly within a 20cm×34cm plane. This study

shows that $\sim 4\%$ of the plane experiences deep fades, confirming multipath fading as a critical cause of performance degradation in WSN. At the same time, the result implies that it would be hard to observe deep fades in general WSN deployment; You must be unfortunate enough to locate a node only at 4% worst area. Our experimental study does not contradict this prior work but reveals that with very high node density, deep fading holes always pop up, which must be addressed. Our contribution is in identifying this problem in a real system.

Some multi-radio diversity techniques have been proposed to mitigate deep fades [9]–[11] in low-power wireless networks and WSN context. For example, Kusy *et al.* [10] proposed a dual radio network architecture and have shown that both cases of dual spaced radio frequencies and spatially separated antennas offer robust communication and improved reliability compared to the case of a single radio. However, they force all (battery-powered) nodes to use multiple radios, which increases not only size and cost of hardware but also energy consumption. In addition, each node pair should cooperatively select a radio for their communication, which increases complexity. In contrast, our diversity techniques require to modify only gateways, which is interoperable with battery-powered nodes designed for single radio operation.

To address multipath fading with normal single-radio hardware, time synchronized channel hopping (TSCH) has been investigated in WSN [14]–[16]. Bluetooth also exploits its own channel hopping technique [17]. Our channel hopping scheme is much simpler than the prior work but effective in ESL environments. In addition, our spatial diversity technique is complementary to the prior work, applying a multi-radio gateway to improve reliability of a channel hopping mechanism without violating its implementation at battery-powered nodes.

III. ESL SYSTEM DESIGN

This section presents the design and implementation of our *ESL* system including its hardware components and protocol operation.

A. SYSTEM REQUIREMENTS

The key requirements of *ESL* mainly come from retailers' feedback and requests [7], [18]:

- **Energy efficiency:** An e-tag should operate for at least 5 years without replacing the batteries since frequent battery replacement may outweigh the cost of paper replacements. Furthermore, it is desirable that all tags have the same (fair) lifetime for ease of management.
- **Reliability:** Neither retailers nor customers tolerate pricing errors. So the e-tags should have up-to-date price information and any inconsistency or error must be timely reported. To achieve this, e-tags should continuously maintain bi-directional connection with the gateway, and the backend server should be aware of any connection and disconnection.

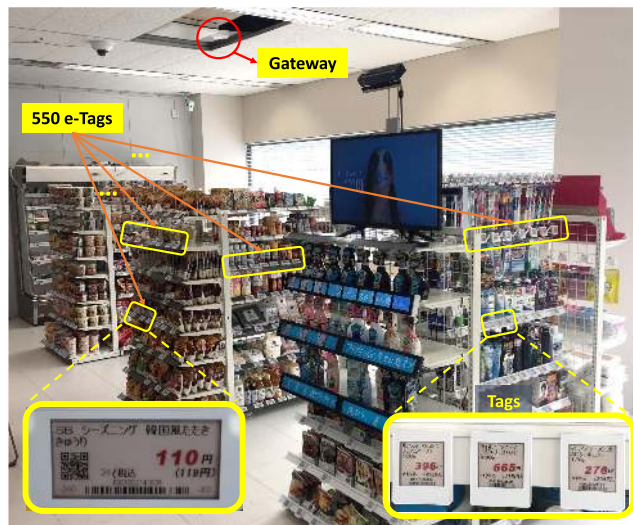


FIGURE 1. A picture of our 550-tag real convenience store deployment. A gateway is mounted on the ceiling, and there are 550 e-tags on the shelves displaying real product information.

- **Scalability:** There could be hundreds to tens of thousands of tags in a store, depending on the number of products and size of the store. This should be covered by a small number of gateways for cost reasons. Thus, one gateway should be able to support at least a few thousands of e-tags.
- **Deterministic operation:** Retailers would like to know deterministically when to expect a response, whether there is an error, and hopefully that everything is fine. Given that probabilistic guarantee is less desired, random contention, random backoff, congestion/rate control, distributed computing, and multihop networking are not preferred.
- **Ease of use:** Store manager is not a computer science expert. The e-tags should work robustly without any manual intervention such as channel number configuration or slot assignment.

Based on these requirements, we have made the following design choices for our hardware, system architecture, and network protocol.

B. MAIN HARDWARE COMPONENTS

There are two types of hardware platform in our *ESL* system; *e-tag* and *gateway*, as illustrated in FIGURE 1. Number of e-tags depends on that of the products in the store. Number of gateways installed depends on the size of the store to cover all the tags (wireless coverage), as well as the number of tags in the store to satisfy desired performance (latency and throughput coverage). Thus, there could be multiple gateways in a large-sized store.

E-tag is a low-cost battery-operated embedded device that maintains wireless connectivity with the gateway, receives updated product information (e.g., name, barcode, and price), if any, and displays it on an electronic screen in the form

of an image.¹ There are e-tags of various sizes and shapes (FIGURE 1) to satisfy the needs of a store, but their essential behaviors are identical. Our e-tag has one low-power TI CC2530 system-on-chip (SoC) which includes an 8-bit microcontroller (MCU) and an IEEE 802.15.4 radio operating on 2.4 GHz ISM band with data rate of 250 kbps and maximum transmission power of 4 dBm. For the display, an e-paper module is used, which consumes energy only when changing the image on the screen. Two AAAA-sized alkaline batteries are used for power supply, providing a total capacity of 500~600 mAh with a goal of lasting a minimum of 5 years.

Gateway maintains connection and communicates with thousands of e-tags. It is also connected to a backend server that manages products and commands tag updates. When there is a need to update/modify the image on a certain e-tag, the gateway (to which that e-tag is connected) receives new images from the server and transmits it to the e-tag. Our gateway hardware design consists of one ARM Cortex-A9 as the main processor, a WiFi and an Ethernet modules for communication with the backend server, and three pairs of a CC2530 SoC and a 15 dB power amplifier for wireless communication. The three IEEE 802.15.4 radios represent *common*, *data*, and *diversity* radios, respectively: (1) *Common* radio operates on a *common* channel for connection maintenance. (2) *Data* radio operates on a *data* channel for transmitting a new image to be displayed on the e-tags. (3) *Diversity* radio is added to enable our proposed enhancements, which we will introduce in Section V-B. We separate the *common* and *data* channel to isolate image download process of a certain e-tag from connection management of all other tags. Lastly, a gateway is wall-powered so that there is no energy constraint, and it is usually attached to the ceiling to maximize its coverage [19], as shown in FIGURE 1.

C. NETWORK ARCHITECTURE

We design a wireless network architecture to satisfy the aforementioned system requirements. The first target environment is a small convenience store but the same architecture can be also applied to larger stores.

Targeting a small store helps to avoid representative technical challenges in the low-power wireless communication: (1) All e-tags are located within the transmission range of the gateway; there is no need for a routing protocol [7], [20]. (2) Although hundreds to thousands of nodes are densely deployed, their throughput requirement is still below the maximum bandwidth (250 kbps in IEEE 802.15.4) considering the practical price update period (~3 times-per-day for a discount item). (3) Since the gateway is wall-powered, the network protocol focuses on energy-efficient operation of only battery-powered e-tags. Therefore, the system design naturally ends up with a *single-hop network* with *radio duty-cycling* protocol.

¹Literally, a .bmp format image

1) DUTY-CYCLING

To satisfy the energy efficiency requirement, e-tags employ radio duty-cycling. Each e-tag wakes up on the *common* channel for a *slot time* T_{slot} , every *sleep interval* T_{sleep} , to maintain connectivity with the gateway (i.e., an exchange of *KeepAlive/Response* messages), and remains in power-saving (sleep) mode for the rest of the time. T_{slot} should be long enough to accommodate a certain number of link-layer retransmissions but an e-tag can fast sleep before the end of T_{slot} if the message exchange is done. The MCU goes into the lowest power consumption sleep mode when the radio sleeps. The values of T_{sleep} and T_{slot} significantly impact the system performance, which is discussed in Section IV-A.

2) SINGLE HOP COMMUNICATION

Our system uses single hop direct communication between a gateway and an e-tag. This was a design choice to minimize the duty-cycle (power consumption) of e-tags, improve the reliability of data delivery, and simplify the protocol for more deterministic behavior. When a target store is too large to be covered by a single gateway, we still maintain this single hop architecture by adding more gateways instead of using multi-hop transmission. This is mainly because multihop networking would require some e-tags to wake up to forward packets on behalf of other e-tags, which would complicate the duty-cycling and consume significant energy in an unbalanced manner. It would also require some form of routing [21] and end-to-end transport protocols [22] for reliable data delivery and connection management.

3) POLLING & SLOT-BASED MAC

Although CSMA is widely used in many wireless systems due to its simple operation, it is known to perform poorly with a large number of contending nodes resulting in high and unpredictable communication delays. In our case, the store manager wants to know for sure whether every node is connected, up-to-date, and responding in a timely and periodic manner when there are thousands of tags connected to a single gateway. For these reasons, we use *slot-based MAC* which eliminates collision and contention issues, providing deterministic operation. Specifically, there are $T_{\text{sleep}}/T_{\text{slot}}$ available slots in the network, and the gateway assigns any empty slot to a newly joining e-tag so that each tag has one timeslot every sleep interval. Note that slot assignment and scheduling is managed by only the gateway (e-tags are dumb followers). Thus, a tag passively sleeps until the next scheduled action, allowing for ultra-low power operation.

In addition, given that all radios of a gateway are always on, we design a *polling-based MAC* where communication between an e-tag and a gateway is always initiated by the e-tag. Each e-tag periodically wakes up at the start of its timeslot (assigned by the gateway), and transmits a *KeepAlive* message to the gateway which polls the gateway and informs the existence and liveness of the e-tag. The gateway responds with a *KeepAliveResponse* message, which includes various

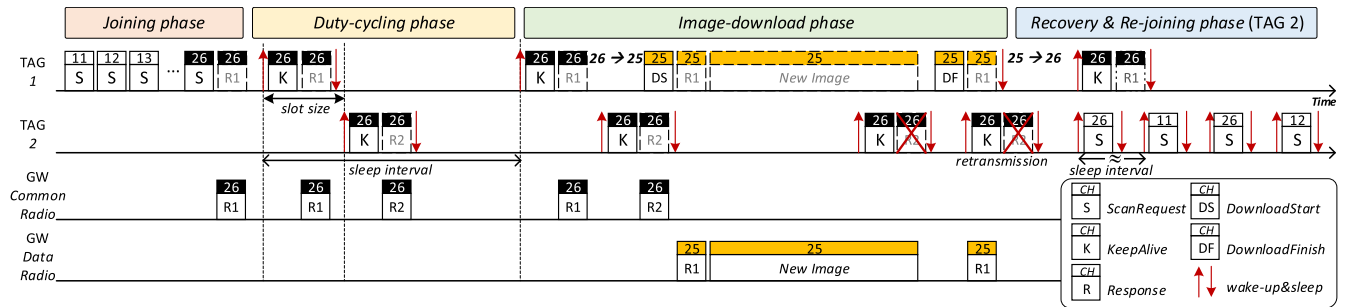


FIGURE 2. Example operation of the communication protocol between two e-tags (TAG-1 and TAG-2) and one gateway in ESL. The gateway uses channel 26 and 25 for common and data channels, respectively.

control information for the e-tag (in Section III-D). Lengths of the *KeepAlive* and response packets are 56~70 bytes, depending on the information each contains.

D. NETWORK PROTOCOL OPERATION

The network protocol operation can be divided into four phases as in FIGURE 2: joining, duty-cycling, image-download, and recovery & re-joining phases.

1) JOINING PHASE

When an e-tag is powered on, it first scans for gateways to join the network. This requires knowing the *common* channels of the gateways² (e.g., channel 26 in FIGURE 2). Having no prior information, an e-tag transmits a batch of *ScanRequest* messages on all the channels sequentially (i.e., from channel 11 to 26). Upon hearing a *ScanRequest* message on the *common* radio,³ a gateway sends a *ScanResponse* message to inform the e-tag of its existence on the *common* channel.

After the scan procedures, the e-tag selects a gateway of the best link quality and transmits a *KeepAlive* message to the gateway. Then the gateway regards the e-tag as ‘connected’, updates the number of connected e-tags, assigns a timeslot (within a sleep interval), and notifies the next polling time to the e-tag by sending a *KeepAliveResponse* message. Upon reception, the e-tag goes to *duty-cycling phase* by activating the polling & slot-based MAC with the next polling time.

2) DUTY-CYCLING PHASE

In duty-cycling phase, each e-tag remains in sleep mode most of the time (T_{sleep}), and wakes up to exchange *KeepAlive/Response* messages with the gateway in its assigned slot on the *common* channel. By using *KeepAliveResponse* message, the gateway informs an e-tag of important events and actions it should take. This includes downloading of new image, channel selection, duty-cycle configuration (T_{sleep}), and scheduling of the next polling time.

²Although the example in FIGURE 2 shows one gateway, there can be multiple gateways around an e-tag depending on store size and deployment choice.

³Note that a gateway does not respond to *ScanRequest* message received on the *data* radio since that is only for unicast image downloads.

Upon receiving a *KeepAliveResponse* and notified of a new image update, the e-tag goes into the *image-download phase*. Otherwise, it remains in the duty-cycling phase and wakes up again at the next slot time notified via the *KeepAliveResponse*. If an e-tag fails to receive a *KeepAliveResponse* message even after a number of attempts (retransmission), it goes into the *recovery phase*.

3) IMAGE-DOWNLOAD PHASE

When the product information to be displayed on an e-tag changes (e.g., bargain sale), the gateway notifies the e-tag using a *KeepAliveResponse* message. Then the e-tag goes to the *image-download phase*, where it switches to the *data* channel (e.g., TAG-1 switches to channel 25 in FIGURE 2) and transmits a download request message to the gateway. Upon receiving the request, the gateway sends the image using the *data* radio.

An image is in.bmp format of size 3500~5600 bytes depending on the display size of the e-tag, and is compressed using run-length-encoding to around 2200~4200 bytes [2]. This is then fragmented into 25~48 packets of 88 bytes each before being transmitted in series as the maximum packet size (including headers) is 127 bytes for IEEE 802.15.4. Any packet loss/corruption is recovered using NACK and retransmissions on the *data* channel until 100% delivery of the image is completed. After receiving all the packets, which usually takes around 500~800 ms, the e-tag combines them to reconstruct, decode, and update the image. After finishing image renewal, the e-tag returns to the duty-cycling phase.

Note that image-downloading on the *data* channel does not interfere with any operation on the *common* channel. For example in FIGURE 2, while TAG-1 is receiving new image fragments from the gateway on *data* channel 25, the others including TAG-2 can still exchange *KeepAlive* messages with the gateway through *common* channel 26.

4) RECOVERY & RE-JOINING PHASE

For various reasons which we will detail in Section V, there is a possibility of failure to exchange *KeepAlive/Response* messages in time. When a tag does not receive a response for its *KeepAlive* message, it retransmits the message within its allocated timeslot T_{slot} . However, T_{slot} may still be insufficient

for multiple retransmissions and eventual reception of a response. In this case, the tag goes into the *recovery phase* in which it decides to retransmit the packets also in the timeslots of other tags. In the recovery phase, e-tag retransmits the *KeepAlive* message up to N_{retx} times (e.g., 5) within a sleep interval T_{sleep} at a regular *retransmission interval* of $T_{\text{sleep}}/N_{\text{retx}}$ until a response is received. To avoid disturbing other e-tags that should exchange messages in their assigned timeslots while retransmitting in the timeslots of those e-tags, retransmissions are done only in the latter half of a slot time T_{slot} , which is designated for retransmissions and recovery. When there is no response from the gateway, the e-tag tries to send a *KeepAlive* message to another gateway on their *common* channel if any was registered during the joining phase. When failing to get any response from all the gateways in the recovery phase, the e-tag goes into the *re-joining phase*.

In the re-joining phase, for only once within one sleep interval, an e-tag scans all the channels by transmitting *ScanRequest* messages. This is done for *fast re-joining* when the *common* channel has been changed. When there is no response from any channel in the *fast re-joining* phase, the e-tag alternates between the last known *common* channel and all other channels from 11 to 26. (e.g., in FIGURE 2, the order is 26, 11, 26, 12, 26, 13... 26, 25, 26, 11 and so on). This alternation takes into account the possibility that the gateway has switched to another *common* channel or still exists on the last known *common* channel. While doing so, for the energy efficiency and to avoid overloading the medium with too many *ScanRequest* messages, the e-tag scans slowly only one channel per sleep interval. If the e-tag succeeds in receiving a response from the gateway on any channel, the e-tag goes back to the *duty-cycling phase* on that channel.

From the gateway's perspective, when there is no *KeepAlive* message from the e-tag for more than K_{thresh} number of *sleep intervals* ($K_{\text{thresh}} \cdot T_{\text{sleep}}$), the gateway regards the e-tag as 'disconnected'. We call this disconnected e-tag an 'Invalid Tag'.

IV. PARAMETER SELECTION AND LIFETIME ANALYSIS

Having described the system architecture and network operation, we discuss the selection of key parameters in *ESL* and estimate the energy consumption and lifetime of an e-tag.

A. PARAMETER SELECTION AT THE GATEWAY

T_{slot} and T_{sleep} are the important parameters in our *ESL* system, which determine e-tag duty-cycle, reliability, price update latency, and scalability (the maximum number of e-tags supported by a gateway, N_{max}). Here we provide some guidelines on how to configure these parameters.

First of all, considering the dynamics of wireless environments, T_{slot} should be long enough to allow for reliable exchange of *KeepAlive/Response* messages (including a few link-layer retransmissions), and also to provide chances for disconnected nodes to scan or re-connect during the '*recover/re-joining phase*' (explained in Section III-D). We set T_{slot} to 150 ms by default, but can be re-configured

considering the wireless environments in which the system is deployed.

With fixed T_{slot} , T_{sleep} should be determined considering the trade-off between latency, duty-cycle, and scalability: (1) As T_{sleep} increases, duty-cycle decreases but latency increases, and (2) every e-tag connected to a gateway should be assigned/guaranteed a timeslot within a *sleep interval*, i.e., $T_{\text{sleep}} \geq N_{\text{max}} \times T_{\text{slot}}$. For our use case (a small store), we set $N_{\text{max}} = 2000$, which results in $T_{\text{sleep}} \geq 5$ min. We use $T_{\text{sleep}} = 5$ min for simplicity, which results in 0.05% duty-cycle. Finally, we use $K_{\text{thresh}} = 3$ which means that an e-tag is regarded as *disconnected* and termed *invalid tag* when there is no communication with that tag for 15 minutes. However, our design enables all these parameters to be *dynamically re-configurable* and controlled at the gateway, and delivered through *KeepAliveResponse* messages without reprogramming e-tags, to meet the application's latency/scalability requirements depending on the size of the store.

B. TAG ENERGY CONSUMPTION AND LIFETIME ESTIMATION

Does this design provide target battery lifetime of 5-years? To answer this, we estimate the energy consumption of an e-tag using the numbers in [23]. An e-tag is in sleep mode most of the time where its current draw is only 1 μA , but wakes up once per sleep interval to exchange messages. Considering the message exchanges and processing delays, on average, the total energy spent (at reference voltage) in duty-cycling phase is 201.64 mA·s per day. When updating an image, the e-tag needs to download an image (13440 mA·ms) and display it on e-paper (15000 mA·ms), resulting in total of 28440mA·ms consumed per image update⁴ Thus, in an ideal scenario with only 3 image updates per day without packet losses, where 99% of the e-tags spend most of their time in duty-cycling phase, an e-tag consumes 286.96 mA·s per day. Since our AAAA battery capacity is 500 mAh, the e-tag's lifetime is estimated to be 17.1 years.

However, this does not take into account packet losses due to wireless communication dynamics. In recovery phase, wasted energy goes up to 6967.33 mA·ms per failed message exchange, and in the (re-)joining phase, additional 1594.73 mA·ms is consumed for exchange of *ScanRequest/Response* messages. If we consider a challenging scenario of 1.5x retransmissions on average (which is much worse than our experimental results), lifetime expectation is still 5.3 years, sufficient to satisfy our goal. The most dominant term for lifetime reduction is the number of failures that result from exchange of *KeepAlive/Response* messages, especially when an e-tag is disconnected ('invalid tag'). Therefore, minimizing the number of failures and disconnected time (recovery time) is critical to e-tag's lifetime which we discuss next in Section V.

⁴Details of calculation omitted for brevity.

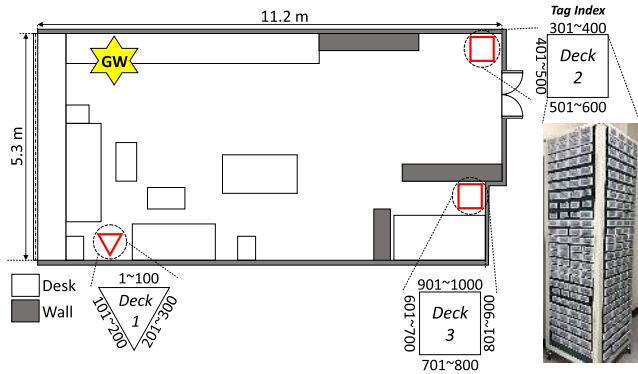


FIGURE 3. In-lab experiment environment with one gateway and 1000 e-tags.

V. CHALLENGES AND ENHANCEMENTS

In this section, we present the observation from our preliminary experimental study and describe the essential enhancements to our system.

A. PROBLEM: ‘DEEP FADING HOLES’

Our work was motivated by complaints from retailers reporting a problem in an existing commercial ESL solution: “a few e-tags, out of thousands, are disconnecting frequently and for long durations, why?”. Issue report was interesting; it was not the distance, not specific nodes but more or less random, and ‘only a few’ out of thousands (small proportion) but ‘always a few’. To identify the problem, we conducted a preliminary study using 1000 e-tags and one gateway, densely deployed on 3 decks in an office of a similar size to a small store as shown in FIGURE 3. Each deck has three or four sides of 1.6m×0.5m, and each side has 100 e-tags with 4 columns and 25 rows. Deck 1 contains tag index from TAG-1 to 300, is located for line-of-sight (LOS) experiment, 3.6 m apart from the gateway. Deck 2 is 8.4 m away from the gateway. A side facing wall (TAG-301 to 400) is Non-line-of-sight (NLOS), the other sides are partially NLOS, hidden from the gateway. Last deck is surrounded by the cabinets representing perfect NLOS environment (TAG-601 to 1000). Transmission power of the gateway is 7 dBm and that of an e-tag is 4 dBm. We use channel 26 for the *common* channel and channel 20 for the *data* channel.

We evaluated e-tag connectivity for a week, confirming that most of the 1000 e-tags are never disconnected from the network during the whole week with high link quality. Specifically, the e-tags on Deck 1 received the gateway signal with received signal strength indicator (RSSI) of -60 to -50 dBm and those on Deck 2 and Deck 3 experience RSSI of -70 to -60 dBm, all of which are much higher than CC2530’s receiver sensitivity, -97 dBm. This verifies that all the e-tags were located close enough to the gateway within its transmission range. On the other hand, surprisingly, several e-tags experienced the *invalid* status (i.e., continuous communication failure for a long time) in this *nice* wireless environment. The proportion of time period during which all 1000 e-tags were connected to the gateway is *only* 25.68%

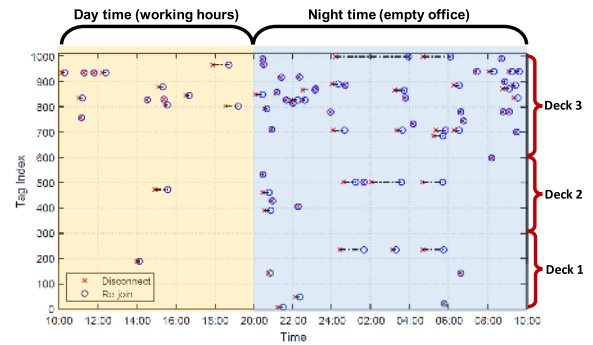


FIGURE 4. Disconnection and re-joining pattern of 1000 e-tags during a weekday.

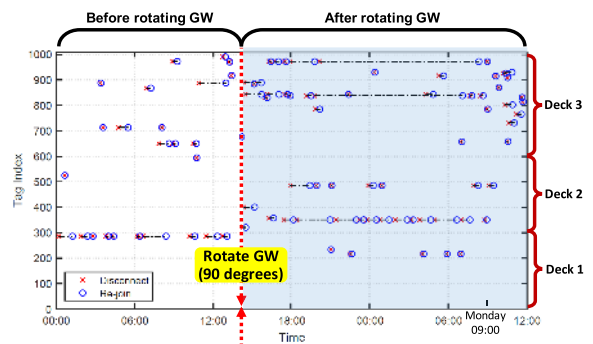


FIGURE 5. Disconnection and re-joining pattern of 1000 e-tags during a weekend. The gateway is rotated 90 degrees on Sunday 3PM.

of the whole week. This severely degrades the applicability of the entire *ESL* system since retailers are sensitive to the occurrence of any invalid tag.

To investigate the reason of disconnection, FIGURE 4 and FIGURE 5 plot when each e-tag is disconnected and re-joins for a weekday and the weekend, respectively. In addition, FIGURE 6 plots the empirical cumulative distribution function (ECDF) of the *recovery time* for invalid tags during the whole week. Interestingly, there are more invalid tags during the night-time and the weekend than the day-time, and the recovery time is also longer as well. While 99% of invalid tags during the day-time are recovered within an hour, *only* 80% of those during the night-time and weekend are recovered within an hour (FIGURE 6). For example, TAG-999 is invalid for 4 hours during the night-time, only to be disconnected again 45 minutes later. This contradicts prior studies [7] which show that the communication performance is worse during the day-time than the night-time due to human activity and WiFi interference. We did confirm that our environment has WiFi interference during the day-time (channel 26 is not WiFi-free in our country), but invalid tags during day-time are recovered quickly.

Then why do more long-disconnected *invalid tags* occur during the night-time and the weekend, despite close distance and stable channel condition without people and WiFi interference? A clue is that the disconnection happens only at a limited set of e-tags, *repetitively*. For example in FIGURE 4, TAG-235, 503 and 999 are repetitively

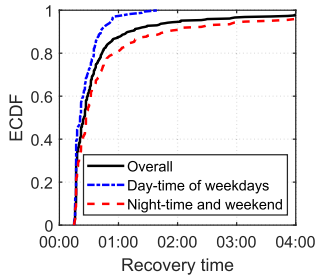


FIGURE 6. ECDF of recovery time of invalid e-tags for a week.

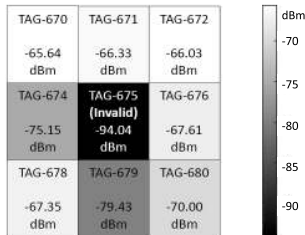


FIGURE 7. RSSI of a frequently disconnected e-tag and its neighbors.

disconnected even though their immediate neighboring devices are 100% connected. This means that the disconnection is related to the e-tag’s position. To clarify the matter, we tried rotating the gateway 90 degrees on Sunday 3PM as marked in FIGURE 5. After the rotation, the disconnection pattern has changed significantly. TAG-286 does not experience disconnection anymore but TAG-351, 486, 839, and 973 started suffering disconnection until Monday morning when people come to the lab. The results confirm that the disconnection depends on the *relative position* between the gateway and the e-tags.

Lastly, FIGURE 7 plots the RSSI of a frequently disconnected e-tag (TAG-675) and its neighboring e-tags, measured at the gateway. Interestingly, these neighboring e-tags, which are only a few centimeters apart from the suffering node, experience much better link quality, 19~27 dBm higher RSSI. This phenomenon seems like only the unfortunate e-tag falling into a disconnection *hole*.

With the above observations, we conclude that multipath fading is the main cause of the problem. Wireless signal from a transmitter is reflected and scattered by objects such as wall, floor, and shelves, generating multipath signals. Signal quality at a receiver largely depends on how these multipath signals are combined. Once they destructively interfere with each other, the receiver experiences *deep fade*, which can even nullify its signal. When scatterers are near to the receiver (metal decks in this case), the multipath combination pattern can change significantly even with a slight position difference [10], resulting in deep fading *holes*.

Interesting fact is that human activity during the day-time, often regarded as a factor of performance degradation [7], causes dynamics on the multipath fading pattern, rescuing an e-tag from a deep fading hole quickly. On the other hand, the stable multipath fading pattern during the night-time and

the weekend causes signal quality at specific locations to be *stably bad*, resulting in more invalid tags. Our study does not contradict prior work [8] but reveals that with very high node density, deep fading holes always pop up, which must be addressed. We see this as a unique finding with *ultra-high* node density, i.e., nodes should be deployed densely enough to uncover possible deep fading holes.

Next, we perform an image update experiment in which the gateway transmits an image to a randomly chosen e-tag, 10~50 e-tags per hour, for 24 hours. The results reveal that image update latency largely depends on e-tag connectivity. Once an e-tag is connected, an image update is completed within 800 ms including some packet loss and retransmissions. However, to update an image on an invalid tag, the gateway can do nothing but wait until the e-tag is connected again (could be more than an hour). Therefore the primary concern for *ESL* system in reality is robust e-tag connectivity.

B. ENHANCEMENTS

To provide robust and reliable connectivity to a large number of densely deployed devices over multipath fading wireless links, we adopt *spatial* and *frequency* diversity techniques with the help of an additional *diversity* radio.

Scheme 1. Spatial Diversity: Given that e-tags are densely deployed on metal shelves in an indoor environment with a number of obstacles, *near-scatter multipath fading model* could be adopted to describe spatial channel characteristics in our *ESL* system. Specifically, when two antennas are physically separated by d_{antenna} , multipath signals from/to these two antennas have correlation ρ , which is represented by using the zero-th order Bessel function [24] as

$$\rho = J_0 \left(\frac{2\pi \times d_{\text{antenna}}}{\lambda} \right) \tag{1}$$

where λ is the wavelength of the signal.

With the value of d_{antenna} that makes correlation ρ zero, these two antennas experience *independent signal quality*: No matter how bad link quality an antenna experiences (e.g., deep fade), it does not affect the other antenna’s link quality. Compared to the single antenna case, possibility that both the two antennas experience deep fades is much lower. Considering the wavelength of 2.4 GHz band, the smallest value nullifying correlation is $d_{\text{antenna}} = 4.6$ cm. For a d_{antenna} value larger than 4.6 cm, correlation is negligible, if not zero. We design the distance between the *common* and *diversity* radio to be 5.3 cm, larger than 4.6 cm, satisfying this requirement.

For the spatial diversity scheme, we use the *diversity* radio as another *common* radio operating on the same *common* channel. The idea is that an e-tag can maintain connectivity when its link to either of the two *common* radios at the gateway does not fall into a deep fading hole. Specifically, when the gateway receives a new message sent from an e-tag via *common* radio 1 (or 2), it responds through that same *common* radio 1 (or 2). If a message is received on both radios, it will be sent out through both radios sequentially. This way,

the gateway can process a packet sent from an e-tag when at least one of the two *common* radios receive it successfully.

From an e-tag's perspective, when it receives any response message, it processes the message and takes required actions (e.g., sleep or change channel to receive a new image). Thus, if an e-tag receives the early-arriving response message, it does not wait for the redundant response message, resulting in no additional energy consumption on e-tags.

Scheme 2. Frequency Diversity: Multipath fading also has frequency selective characteristic, which is caused by differences in the times of arrival of multiple signals. Two channels separated larger than coherence bandwidth provide independent link quality. The coherence bandwidth $B_{\text{coherence}}$ is determined depending on $\tau_{\text{dispersion}}$ (arrival time difference between radio signals) as [10]

$$B_{\text{coherence}} = \frac{2\pi}{\tau_{\text{dispersion}}}, \quad (2)$$

and thus separation of three IEEE 802.15.4 channels (i.e., 15 MHz) is enough to get independent link quality in an indoor environment [8].

We combine the two diversity techniques into our design. We use the *diversity* radio as another *common* radio operating on a different channel, *common* channel 2 per se, where the two *common* channels are separated by more than 15 MHz. Since the two *common* radios operate on different channels, the gateway can transmit two responses independently. When the gateway receives a new message sent from an e-tag via *common* radio 1 (or 2), it responds through the same radio. An e-tag should have found at least one or both channels during the *join* phase, and will use whichever that works. In this way an e-tag and the gateway can communicate with high probability when at least one of the two *common* radios are not in a deep fading hole. The idea is that an e-tag can maintain connectivity when its link to either of the two *common* radios separated by some physical/frequency distance at the gateway does not fall into a deep fading hole.

An e-tag should be able to know both *common* channel 1 and 2 during the joining phase. Assume that it joins the *common* channel 1 but the channel falls into a deep fading hole, resulting in continuous message exchange failures even in the recovery phase. Then, the e-tag tries to exchange *KeepAlive/Response* on the *common* channel 2 before going to the re-joining phase, which can re-establish connection with high probability. Scheme 2 is expected to outperform Scheme 1 since it benefits from both spatial and frequency diversity.

VI. PERFORMANCE EVALUATION

In this section, we evaluate the performance of our *ESL* system at a real convenience store in FIGURE 1, with and without the enhancements developed in Section V-B. The store was closed during the experiments, providing a stable wireless environment. We deployed 550 e-tags on 4 shelf-racks with 13 sides in the convenience store. Depending on the number of items on the shelves, each side of a shelf has

TABLE 1. Connectivity performance of in-store experiments.

	Without enhancements	Scheme 1 (Gain)	Scheme 2 (Gain)
Network Connectivity	17.76%	87.85% (4.9x)	98.51% (5.5x)
Disconnection duration (/day)	19:44:11	2:55:50 (85.2%)	0:07:08 (99.4%)
Avg. # of different invalid tags (/day)	13	4.67 (64.1%)	0.33 (97.5%)
Avg. # of disconnection events (/day)	29.7	5.33 (82.1%)	0.33 (98.9%)

14~67 e-tags on 2~8 rows. One gateway is attached to the ceiling, close to the center of all shelves, and is connected to the backend server through Ethernet. The height of the ceiling is 2.93 m, and the distance between the gateway and the farthest e-tag is at most 5 m. Transmission power is set to 10 dBm for the gateway and 4 dBm for the e-tags. Channel 26 and 25 are used for the *common* and *data* channel, respectively. We confirmed that there is no other network (including WiFi) operating on channel 26. For the frequency diversity scheme, channel 23 is used for the *diversity* radio. Each experiment ran for 3 days.

We define *network connectivity* as the percentage of time during which *all e-tags* are connected to the gateway, and TABLE 1 compares the performance of the schemes with/without enhancements. Without diversity schemes, *ESL*'s connectivity is only 17.76%, even worse than the result from our in-lab experiment (25.68%); for almost 20 hours per day, at least one e-tag was invalid. The low performance confirms that the results of our in-lab experiments are reproducible. On the other hand, applying diversity schemes provides remarkable performance improvement. Scheme 1 and Scheme 2 achieve 87.85% and 98.51% of connectivity, respectively. Specifically, compared to the basic scheme, the number of e-tags experiencing disconnection decreases by 64.1% and 97.5%, respectively. The number of disconnection events is also significantly reduced. This verifies the impact of both spatial and frequency diversity on deep fading mitigation.

Given that the system's applicability depends on the worst performing e-tags, we take a deeper look into the behavior of e-tags which experience the invalid status at least once. FIGURE 8(a) plots recovery time of invalid tags. The basic scheme experiences much longer recovery time than the others. Specifically, among the invalid e-tags, 35.7% fail to re-join for more than 1 hour, 10.1% are disconnected for even more than 4 hours, and the worst e-tag is invalid for 16 hours. In contrast, 92% of invalid tags re-join in 1 hour with Scheme 1 and 100% of those re-join in 22 minutes with Scheme 2. With this significantly shorter recovery time, both diversity schemes improve the latency and lifetime performance of the worst-case e-tag. In addition, FIGURE 8(b) presents the number of e-tags according to disconnection frequency. It shows that the diversity schemes successfully prevent an e-tag from experiencing multiple disconnections, even zero in the case of Scheme 2. This helps to minimize

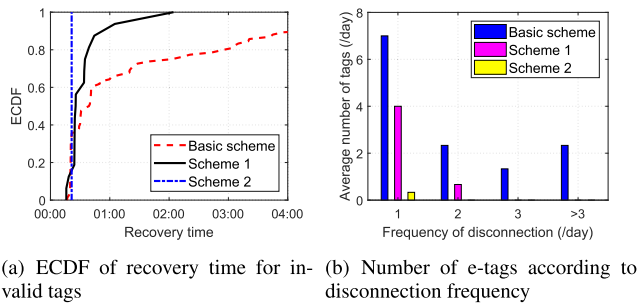


FIGURE 8. Performance comparison of the ESL design, with and without the spatial and frequency diversity scheme, from in-store experiments for 3 days.

lifetime degradation of the worst-performing e-tags, resulting in less management cost.

Lastly, although figures are omitted due to the space limit, we observed 369~1845 ms of image update latency (590 ms on average) for 1050 trials with randomly chosen e-tags. This high variation comes from various image sizes and link quality. In addition, we observed connectivity performance improvement when a store opens and includes human activity, which coincides with the results in Section V-A.

Overall, the results show that the diversity schemes nearly *eliminate* the deep fading problem. Although few e-tags still suffer deep fades, these e-tags are rescued fast and much less likely to suffer again. Scheme 2 outperforms Scheme 1, verifying that more diversity results in better performance. If we change the definition of connectivity to the average percentage of time period during which each e-tag is connected to the gateway, then we achieve 99.94% with Scheme 2. Although the current version has one *diversity* antenna, using more antennas will improve performance further.

VII. CONCLUSION

We presented a real commercial-ready *electronic shelf labeling system* for today's and future markets. We made natural design choices in the light of two decades of research, aiming to satisfy reliability, latency, lifetime, and scalability requirements of ESL system. For thorough investigation of its applicability, we have gone through hardware manufacture, software implementation, and large-scale (up to 1000 e-tags) system deployments. With all of these efforts, it was shown that a low-power wireless system with *ultra-high node density* in *scatter-rich* indoor environments almost always has some nodes floundering in *deep fading holes*. It turned out that simple spatial/frequency diversity techniques are enough to alleviate the problem, providing 98.51% network connectivity, 99.94% average node connectivity, <1850 ms latency for image update, and 5 years of lifetime. Even in a small store, employing these techniques is not optional but a must for practical system operation. This study bridges academia and industry, and shows that the real world could serve as the best model to investigate practical wireless communication problems. We believe that our findings provide practical

lessons learned for wireless system developers, and our system is now under massive production for deployment at more convenience stores. Although our ESL solution was tested in a small convenience store, this can be a building block for a larger store deployment. As our future work, we plan to expand our system to several tens of thousands of e-tags with multiple gateways for an *ultra-large-scale* low-power wireless network.

REFERENCES

- [1] R. Szweczyk, A. Mainwaring, J. Anderson, and D. Culler, "An analysis of a large scale habitat monitoring application," in *Proc. ACM Int. Conf. Embedded Netw. Sensor Syst. (SenSys)*, Nov. 2004, pp. 214–226.
- [2] J. Paek, J. Hicks, S. Coe, and R. Govindan, "Image-based environmental monitoring sensor application using an embedded wireless sensor network," *Sensors*, vol. 14, no. 9, pp. 15981–16002, 2014.
- [3] J. Park, W. Nam, J. Choi, T. Kim, D. Yoon, S. Lee, J. Paek, and J. Ko, "Glasses for the third eye: Improving the quality of clinical data analysis with motion sensor-based data filtering," in *Proc. ACM Int. Conf. Embedded Netw. Sensor Syst. (SenSys)*, Nov. 2017, pp. 1–8.
- [4] M. Garaus, E. Wolfsteiner, and U. Wagner, "Shoppers' acceptance and perceptions of electronic shelf labels," *J. Bus. Res.*, vol. 69, no. 9, pp. 3687–3692, 2016.
- [5] J. G. Evans, R. A. Shober, S. A. Wilkus, and G. A. Wright, "A low-cost radio for an electronic price label system," *Bell Labs Tech. J.*, vol. 1, no. 2, pp. 203–215, Autumn 1996.
- [6] K. Yu, Z. Xie, J. Qian, and G. Jin, "The implementation of electronic intelligent tag system based on wireless sensor network," *Commun. Netw.*, vol. 5, no. 1, p. 39, 2013.
- [7] H.-S. Kim, H. Cho, M.-S. Lee, J. Paek, J. Ko, and S. Bahk, "MarketNet: An asymmetric transmission power-based wireless system for managing e-price tags in markets," in *Proc. ACM Int. Conf. Embedded Netw. Sensor Syst. (SenSys)*, Nov. 2015, pp. 281–294.
- [8] T. Watteyne, S. Lanzisera, A. Mehta, and K. S. Pister, "Mitigating multipath fading through channel hopping in wireless sensor networks," in *Proc. IEEE Int. Conf. Commun. (ICC)*, May 2010, pp. 1–5.
- [9] J. Gummeson, D. Ganesan, M. D. Corner, and P. Shenoy, "An adaptive link layer for range diversity in multi-radio mobile sensor networks," in *Proc. IEEE INFOCOM*, Apr. 2009, pp. 154–162.
- [10] B. Kusy, "Radio diversity for reliable communication in WSNs," in *Proc. 10th IEEE Int. Conf. Inf. Process. Sensor Netw. (IPSN)*, Apr. 2011, pp. 270–281.
- [11] A. B. M. Alim Al Islam, M. S. Hossain, V. Raghunathan, and Y. C. Hu, "Backpacking: Energy-efficient deployment of heterogeneous radios in multi-radio high-data-rate wireless sensor networks," *IEEE Access*, vol. 2, pp. 1281–1306, Nov. 2014.
- [12] C. A. Boano, S. Duquennoy, A. Förster, O. Gnawali, R. Jacob, H.-S. Kim, O. Landsiedel, R. Marfievici, L. Mottola, G. P. Picco, X. Vilajosana, T. Watteyne, and M. Zimmerling, "IoT-Bench: Towards a benchmark for low-power wireless networking," in *Proc. CPSBench Workshop*, Apr. 2018, pp. 36–41.
- [13] J. Hill, R. Szweczyk, A. Woo, S. Hollar, D. Culler, and K. Pister, "System architecture directions for networked sensors," *ACM SIGOPS Oper. Syst. Rev.*, vol. 34, no. 5, pp. 93–104, Nov. 2000.
- [14] A. Elsts, S. Duquennoy, X. Fafoutis, G. Oikonomou, R. Piechocki, and I. Craddock, "Microsecond-accuracy time synchronization using the IEEE 802.15.4 TSCH protocol," in *Proc. IEEE LCN Workshops*, Nov. 2016, pp. 156–164.
- [15] S. Duquennoy, B. A. Nahas, O. Landsiedel, and T. Watteyne, "Orchestra: Robust mesh networks through autonomously scheduled TSCH," in *Proc. ACM Conf. Embedded Netw. Sensor Syst. (SenSys)*, Nov. 2015, pp. 337–350.
- [16] S. Duquennoy, A. Elsts, B. A. Nahas, and G. Oikonomo, "TSCH and 6TISCH for Contiki: Challenges, design and evaluation," in *Proc. Int. Conf. Distrib. Comput. Sensor Syst. (DCOSS)*, Jun. 2017, pp. 11–18.
- [17] S.-H. Lee, H.-S. Kim, and Y.-H. Lee, "Mitigation of co-channel interference in Bluetooth piconets," *IEEE Trans. Wireless Commun.*, vol. 11, no. 4, pp. 1249–1254, Feb. 2012.
- [18] H.-S. Kim, J. Ko, and S. Bahk, "Smarter markets for smarter life: Applications, challenges, and deployment experiences," *IEEE Commun. Mag.*, vol. 55, no. 5, pp. 34–41, May 2017.

[19] R. Elhabyan, W. Shi, and M. St-Hilaire, “Coverage protocols for wireless sensor networks: Review and future directions,” *J. Commun. Netw.*, vol. 21, no. 1, pp. 45–60, Feb. 2019.

[20] S. Jeong, E. Park, D. Woo, H.-S. Kim, J. Paek, and S. Bahk, “MAPLE: Mobility support using asymmetric transmit power in low-power and lossy networks,” *J. Commun. Netw.*, vol. 20, no. 4, pp. 414–424, 2018.

[21] H.-S. Kim, J. Ko, D. E. Culler, and J. Paek, “Challenging the IPv6 routing protocol for low-power and lossy networks (RPL): A survey,” *IEEE Commun. Surveys Tuts.*, vol. 19, no. 4, pp. 2502–2525, 4th Quart., 2017.

[22] M. Park and J. Paek, “TAiM: TCP assistant-in-the-middle for multihop low-power and lossy networks in IoT,” *J. Commun. Netw.*, vol. 21, no. 2, pp. 188–195, 2019.

[23] *A True System-On-Chip Solution for 2.4-GHz IEEE 802.15.4 and ZigBee Applications*, document CC2530 datasheet, Texas Instruments, Feb. 2011.

[24] A. Goldsmith, *Wireless communications*. Cambridge, U.K.: Cambridge Univ. Press, 2005.



JINWOO OCK received the B.S. degree in electrical engineering and the Ph.D. degree in electrical engineering and computer science from Seoul National University, in 2011 and 2019, respectively. His research interests include designing protocols for the Internet of Things (IoT) systems and managing Cross Technology Interference (CTI) in the ISM bands.



HONGCHAN KIM received the B.S. degree in electrical engineering from Seoul National University, in 2015. He is currently pursuing the Ph.D. degree with the School of Electrical and Computer Engineering, Seoul National University, Seoul, South Korea. His research interests include designing routing protocols for low power networks and constructing the mobile IoT systems. He received the National Research Foundation (NRF) Global Ph.D. Fellowship, in 2016.



HYUNG-SIN KIM received the B.S. degree in electrical engineering and the M.S. and Ph.D. degrees in electrical engineering and computer science from Seoul National University (SNU), South Korea, in 2009, 2011, and 2016, respectively. From March 2016 to August 2016, he was a Postdoctoral Researcher with the Network Laboratory (NETLAB), SNU, led by Dr. Saewoong Bahk. He is currently a Postdoctoral Researcher with the Software-Defined Building (SDB) Group, University of California, Berkeley, led by Dr. David E. Culler. His research interests include the development of the IoT systems for urban marketplaces, smart grid and SDB, and network and communication protocols for low-power wireless systems.



JEONGYEUP PAEK received the B.S. degree from Seoul National University, in 2003, and the M.S. degree from the University of Southern California, in 2005, both in electrical engineering, and the Ph.D. degree in computer science from the University of Southern California (USC), in 2010, where he was a member of the Networked Systems Laboratory (NSL), led by Dr. Ramesh Govindan. He was with Deutsche Telekom Inc. R&D Labs, USA, as a Research Intern, in 2010, and then joined Cisco Systems Inc., in 2011, where he was a Technical Leader in the Internet of Things Group, Connected Energy Networks Business Unit (formerly the Smart Grid Business Unit). In 2014, he was an Assistant Professor with the Department of Computer Information Communication, Hongik University. He is currently an Associate Professor with the School of Computer Science and Engineering, Chung-Ang University, Seoul, South Korea.



SAEWOONG BAHK received the B.S. and M.S. degrees in electrical engineering from SNU, in 1984 and 1986, respectively, and the Ph.D. degree from the University of Pennsylvania, in 1991. He was the Director for the Institute of New Media and Communications, from 2009 to 2011. Prior to joining SNU, he was with the AT&T Bell Laboratories as a member of Technical Staff, from 1991 to 1994, where he had worked on network management. He is currently a Professor with Seoul National University (SNU). He has been leading many industrial projects on 3G/4G/5G and the IoT connectivity supported by Samsung Electronics, LG Electronics, SK Telecom, etc. He published more than 200 technical articles and holds 72 patents. He is a member of Who’s Who Professional in Science and Engineering. He received KICS Haedong Scholar Award, in 2012. He was a TPC Chair for IEEE VTC-Spring 2014 and a General Chair of JCCI 2015. He is a Co-EiC of IEEE/KICS JOURNAL OF COMMUNICATIONS AND NETWORKS (JCN), and was on the Editorial Board for *Computer Networks Journal* (COMNET) and the IEEE TRANSACTIONS ON WIRELESS COMMUNICATIONS (TWireless).

...